OCTOBER 03 2024

A comparison of modeled and measured impedance of brass instruments and their mouthpieces and bells FREE

Miranda Jackson; Gary Scavone

Proc. Mtgs. Acoust. 54, 035004 (2024)
https://doi.org/10.1121/2.0001925

Proceedings of Meetings on Acoustics

Volume 54 http://acousticalsociety.org/

Acoustics Week in Canada

Joint Meeting
186th Meeting of the Acoustical Society of America
and the Canadian Acoustical Association

Ottawa, Ontario, Canada
13-17 May 2024

***Musical Acoustics: Paper 2aMU2**

A comparison of modeled and measured impedance of brass instruments and their mouthpieces and bells

Miranda Jackson and Gary Scavone
Schulich School of Music, CIRMMT, McGill University, Montreal, QC, H3A 1E3, CANADA; miranda.jackson@mail.mcgill.ca; gary.scavone@mcgill.ca

Several techniques for modeling and measuring the impedances of mouthpieces and flaring bells of brass instruments (in this case, a trumpet) are presented. A method for isolating the measured instrument impedance without a mouthpiece is described. The ultimate goal is to be able to use transfer matrix techniques to model a full brass instrument. Additionally, methods for characterizing mouthpieces from both model and measurement are outlined, along with a parameterization of the inner geometry of the mouthpiece. Results of transfer matrix and finite element calculations for isolated mouthpieces are found to match each other well, though there is room for improvement regarding the agreement between calculation and measurement, most likely due to uncertainty in the geometry. The calculation of transfer matrix elements from impedance measurements is promising, but is also affected by uncertainty in the geometry of the end condition. Several different impedance calculations have been compared with a measurement of a 3D-printed scale model of a trumpet bell. There is very good agreement between calculation and measurement using the finite element technique, and the transfer matrix technique is found to match best when pulsating sphere radiation and segment lengths corresponding to spherical wave propagation are taken into account.

***POMA Student Paper Competition Winner**

Published by the Acoustical Society of America

 https://doi.org/10.1121/2.0001925

1. INTRODUCTION

The input impedance of a brass instrument is a measure of the quotient of acoustic pressure to volume flow at the inlet. This relation, which is complex and varies with frequency, can be used for evaluating the quality of the instrument and as a starting point for playing simulations and playability studies. The transfer matrix method (described briefly in §2.A) allows for the calculation of the impedance of individual components along the air column. Therefore, once the contributions from all instrument components are known, they can be combined into a calculation of the input impedance for the entire instrument.

In comparison to the plethora of publications regarding the impedance, playability, design, and other aspects of brass instruments, there are relatively very few recent publications regarding mouthpieces individually or specifically (e.g., Plitnik and Lawson, 1999; Poirson et al., 2005; Zicari et al., 2013) or the bell (e.g., Campbell et al., 2013; Eveno et al., 2012; Hélie and Rodet, 2003; Macaluso and Dalmont, 2011; Pyle, 1975; Webster, 1949). This is surprising, given how important these components are considered by players to be. This work is intended as a continuation of the effort into investigating the acoustic effects of mouthpiece geometry and bell shape and radiation.

The models used in this paper are described in §2. The various types of characterizations of individual instrument components are discussed in §3. Results and conclusions can be found in §4 and are discussed in §5.

2. MODELS USED

A. TRANSFER MATRIX METHOD

The transfer matrix method (TMM) involves a calculation in the frequency domain for each segment of a one-dimensional air column, by considering it as either a cylinder or a cone, shapes for which we have analytic characterizations. Matrix multiplication is used to combine the segments in order from the outlet to the inlet, starting from the load impedance at the outlet, Z_L. The result of this calculation is the input impedance Z_{in}.

The matrix equation for each segment is given by:

$$\begin{bmatrix} P_0 \\ U_0 \end{bmatrix} = \begin{bmatrix} a & b \\ c & d \end{bmatrix} \begin{bmatrix} P_L \\ U_L \end{bmatrix} \tag{1}$$

where P_0 and U_0 are the pressure and volume velocity at the inlet of each segment, P_L and U_L are those at the outlet, corresponding to the load, and a, b, c, and d are the elements of the transfer matrix for that particular segment. The segment in question could be a cylinder or a cone, or because the matrices for many small cylindrical or conical segments can be combined through multiplication, the segment in question could be an entire mouthpiece or another contiguous section of an instrument. Since impedance is pressure divided by volume velocity, Eq. 1 can also be written as

$$Z_{\text{in}} = \frac{b + aZ_L}{d + cZ_L} \tag{2}$$

where each parameter in the equation is a function of frequency and complex to allow for viscothermal losses near the walls.

For the calculations of the viscothermal losses, the "wide-pipe" approximation (Keefe, 1984) could be used, but we have instead opted to use the expressions involving Bessel functions (Chaigne and Kergomard, 2016). We expect these to be more accurate, given the narrow radius of the throat of the trumpet mouthpiece.

B. FINITE ELEMENT METHOD

The finite element method (FEM) involves building a mesh along the edges of an acoustical domain and applying physical principles to the airflow and pressure at each small volume element. The "wall admittance" (Chaigne and Kergomard, 2016; Cremer, 1948) is used for the losses.

The calculations are performed with COMSOL. An axisymmetric geometry is used for all results presented here, and the mesh comprises triangular elements with dimensions between 0.001 and 0.5 mm. An incident pressure field is used at the inlet. The resulting input impedance is the pressure divided by the volume velocity at the inlet.

3. CHARACTERIZATION OF INDIVIDUAL INSTRUMENT COMPONENTS

A. INSTRUMENT LOAD IMPEDANCE

When working on modeling mouthpieces, it is useful to be able to characterize the load impedance seen by a mouthpiece that is attached to the instrument. This is difficult to measure directly because the impedance measurement would need to be made at the point to which the end of the mouthpiece extends into the instrument leadpipe, but it can nevertheless be calculated from the result of a single impedance measurement.

For this purpose, a Vincent Bach Model 37 ML trumpet was attached to the impedance probe with a 3D printed cylindrical adaptor (shown in Fig. 1) that can be inserted into a trumpet leadpipe similarly to a mouthpiece. Removing the mouthpiece from the impedance measurement isolates the impedance of the instrument itself. The adaptor can be decoupled from the measured impedance by solving Eq. 2 for Z_L, once its transfer matrix elements are calculated with TMM. Because the adaptor has the inner geometry of a single cylinder, it is straightforward to model its effect on the impedance.

***Figure 1:** Wire diagram of the 3D printed cylindrical adaptor used for impedance measurements.*

Once the load impedance is obtained, it can be "virtually" combined with a mouthpiece for which the transfer matrix elements are known or can be calculated through an application of Eq. 2. This technique can be used both to model the load impedance of an entire instrument and to characterize the load impedance for a mouthpiece under various measurement conditions, as described in §3.B.iii.

B. MOUTHPIECES

i. Parameterizing mouthpiece geometry

It is useful to be able to parameterize the inner geometry of a brass mouthpiece in order to evaluate the effect on the impedance of changing one of the parameters in isolation. To this end, the parameterization shown in Fig. 2 is proposed.

In this work, Vincent Bach 5C and $1\frac{1}{2}$C trumpet mouthpieces, for which the geometries have been accurately measured, have been parameterized. The result of this parameterization is shown in Fig. 3. The 5C parameterization has also been modified as described in the caption, to test the effect of the modification on the impedance.

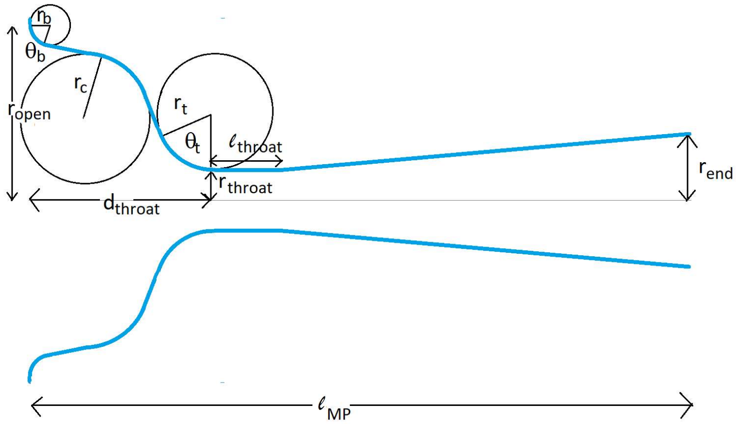

Figure 2: Proposed parameterization of a trumpet mouthpiece.

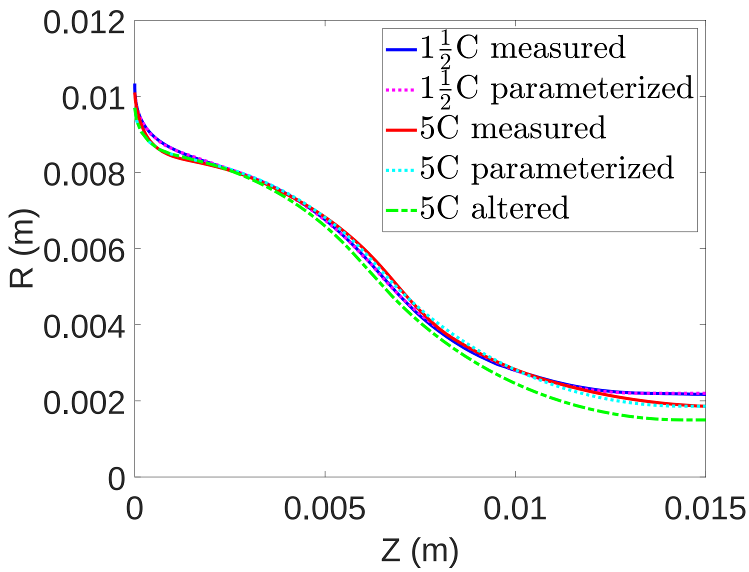

Figure 3: Measured geometries and parameterizations of Vincent Bach 5C and $1\frac{1}{2}$C trumpet mouthpieces, and a modification of the 5C mouthpiece parameterization produced by narrowing just the throat radius and leaving all other parameters unchanged. R is the radial dimension and Z is the dimension along the axis.

ii. Approximating the mouthpiece cup

In the literature, the mouthpiece is often treated as a lumped element with a given volume that changes the effective length of the overall instrument at frequencies above its own resonance frequency (Ayers, 1996; Backus, 1977; Mignot et al., 2010; Zicari et al., 2013). The model of a mouthpiece cup as a cylindrical or a conical volume element has been tested and compared with a model using more precise geometry and with an impedance measurement.

Figure 4 shows approximations of the 5C mouthpiece in which the cup has been replaced by a single cylinder or a single cone. In both cases, the volume and opening radius are maintained. For the case of the cone, the cup depth is also the same as the original.

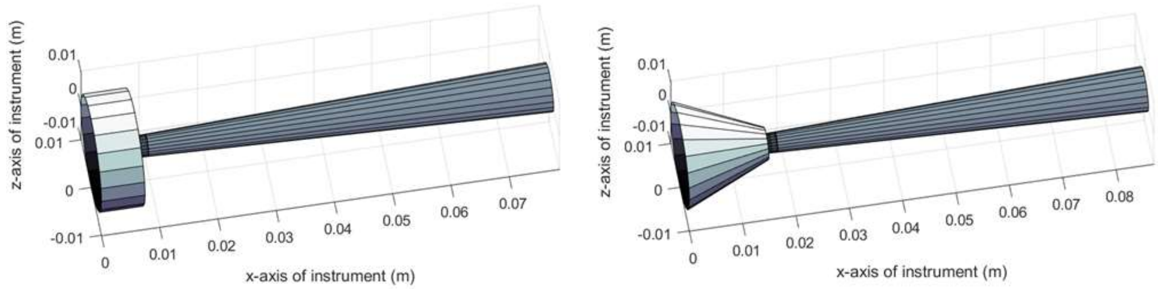

Figure 4: Wire diagrams of a cylindrical (left) and conical (right) approximation of the cup of the 5C mouthpiece described in §3.B.ii.

iii. Calculating mouthpiece transfer matrix elements from impedance measurements

Given Eq. 2, it is hypothesized that if the input and load impedances are known, the transfer matrix elements could be calculated from the impedance measurements of a mouthpiece with three different loads. The fact that Eq. 2 involves a quotient requires only that three of the matrix elements be known as a multiple of the fourth (for each frequency), in order to calculate the input impedance curve of a known load connected to the mouthpiece in question. For this reason, only three linear equations are required.

The load impedance corresponding to any given measurement with a mouthpiece is calculated from an impedance measurement with the cylindrical adaptor pictured in Fig. 1 replacing the mouthpiece in the same configuration: open, closed, or with any other load at the outlet. The procedure given in §3.A is used to isolate the load impedance for each measurement. Therefore, six impedance measurements are required in total: three of the mouthpiece with different loads, and three of the cylindrical adaptor with those same loads. Since Z_{in} and Z_L are both known quantities for each pair of impedance measurements, this leads to three unknowns for each of three instances of Eq. 2, each of which can be written as a linear equation involving three matrix element ratios.

A study has been done as to the requirements for the three loads most conveniently employed for this effort. It is reasonable to start with open and closed ends for two of the impedance measurements, which necessitates only one more measurement to determine the matrix elements. Both a full trumpet and the bell shape shown in Fig. 5 were considered as a potential third load. However, it was found that the b element is highly sensitive to the load impedance that is used, even when simulated “impedance measurements” calculated using TMM are used. The initial calculations indicated that a load with very little variation over frequency is required. Thus, it was determined that an anechoic end is ideal for the third load.

To simulate an anechoic end, the anechoic condition used to calibrate the probe is used. This is a 30 m long plastic tube intended for plumbing applications. To use this load, a 3D printed coupler is used to connect the mouthpiece to the pipe for the first impedance measurement, and then the cylindrical adaptor to the pipe for the next measurement. The load impedance is calculated using the latter of these measurements, again following the procedure in §3.A.

Once the input impedances (from the direct mouthpiece impedance measurements) and the load impedances (calculated from the measurements with the cylindrical adaptor) are known with the three loads, it is relatively straightforward to use the three different instances of Eq. 2 to solve for the matrix element ratios.

This was first done by assuming an infinite load impedance for the closed end, which results in ratios of a, b, and d relative to c (and requires only five impedance measurements rather than six), but if the load impedance for the closed end condition is determined from a measurement with the cylindrical adaptor, the most straightforward algebraic rearrangement results in the elements relative to a instead. The final result was found to be of approximately similar quality by using either method, and is shown in §4.B.ii.

C. THE BELL

As with mouthpieces, the geometry of a flaring bell is rather difficult to measure without specialized equipment. Moreover, this study would ideally require the use of a trumpet bell without the rest of the instrument attached, which was not available. Therefore, we opted to 3D print a 1:2.5 scale model of a trumpet bell, shown in Fig. 5. The geometry for this model was taken from Jansson and Benade (1974) (the third trumpet bell). For convenience, the 3D printed shape fits onto the end of a trumpet mouthpiece or onto the end of the cylindrical adaptor shown in Fig. 1.

Figure 5: Wire diagram of the 3D printed trumpet bell shape used for impedance measurements.

To model the impedance of the bell shape attached to the cylindrical adaptor, four modeling methods were used:

1. TMM with cylindrical or conical segments as appropriate and an unflanged end (Dalmont, 2001).
2. Same as above, but with the radiation model for the pulsating sphere (Eveno et al., 2012; Hélie and Rodet, 2003) in place of the unflanged end.
3. Same as above, but with the spherical wave shape in the conical components accounted for with an adjustment in the length parameter of the segments from the axial lengths to the lengths along the conical walls, as suggested by Eveno et al. (2012).
4. A finite element model (COMSOL) calculation with an axisymmetric geometry and a small radiating volume, including the outer wall of the 3D printed "bell" shown in Fig. 5.

4. RESULTS AND CONCLUSIONS

A. LOAD IMPEDANCE

To evaluate the efficacy of the method described in §3.A, the load impedance of the trumpet was calculated from an impedance measurement with the cylindrical adaptor. This was then combined with a TMM calculation from the accurate geometry of a Vincent Bach 5C mouthpiece using Eq. 2. A second impedance measurement was made with the same trumpet attached to the impedance probe with the 5C mouthpiece.

The results are shown in Fig. 6. It is clear from the similar shapes of the curves that the measured impedance is qualitatively matched quite accurately by means of this method. Any deviation that is observed would be expected to arise from both uncertainty in the mouthpiece geometry and from the fact that the cylindrical adaptor may enter the instrument leadpipe to a different depth than the mouthpiece. This is to be expected because mouthpieces do have slightly varying outer geometries, and it would amount to a slight overall length difference when another mouthpiece (or the adaptor, in this case) is used in place of a given

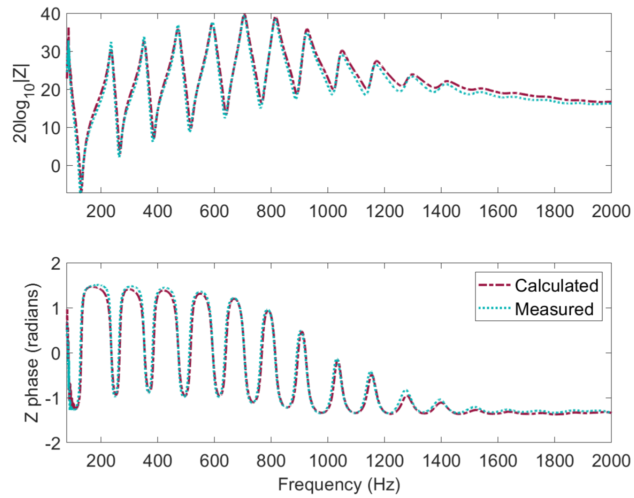

Figure 6: A comparison of the impedance (magnitude and phase) determined from a TMM calculation from the mouthpiece geometry combined with the trumpet load impedance (described in §3.A), and a direct impedance measurement of the same trumpet and mouthpiece combination.

mouthpiece. It will be the subject of a future study to determine the impact of this effect and how to remove it from the result.

B. MOUTHPIECE IMPEDANCE

i. Impedance from geometry

Comparisons of impedance calculations from the various calculation methods and geometries (described in §2, §3.B.i, and §3.B.ii) with an impedance measurement are shown in Fig. 7. The legends show the identities of the various curves.

It can be seen that the TMM impedance calculations from the original geometry and from the parameterization, as well as the FEM (COMSOL) calculation match well, at least qualitatively, with the impedance measurement (black) with zProbe (Lefebvre and Scavone, 2011). The modeled impedance from the approximated cup geometries (green and orange) are seen to deviate increasingly at high frequencies. The altered geometry (light blue) discussed in §3.B.i (with a narrower throat) produces an impedance curve with a notably different position of the first peak, which would make a difference in the envelope of the trumpet impedance as well.

ii. Matrix elements from impedance measurements

The results of the calculations of the matrix elements from impedance measurements (described in §3.B.iii), along with those calculated with TMM from the geometry, for the 5C mouthpiece, are shown in Fig. 8. It can be seen that the general shapes and peak heights are matched, but there are some mismatches in the peak positions in frequency.

The calculated and measured overall trumpet impedances are shown in Fig. 9. From a visual examination of the curves, it can be seen that, as before, the matrix elements calculated with TMM from the mouthpiece geometry and then combined with the load impedance (yellow curve) match the measured input impedance (blue curve) quite well, but there is a significant deviation in the input impedance calculated from the "measured" matrix elements (red curve) above around 800 Hz.

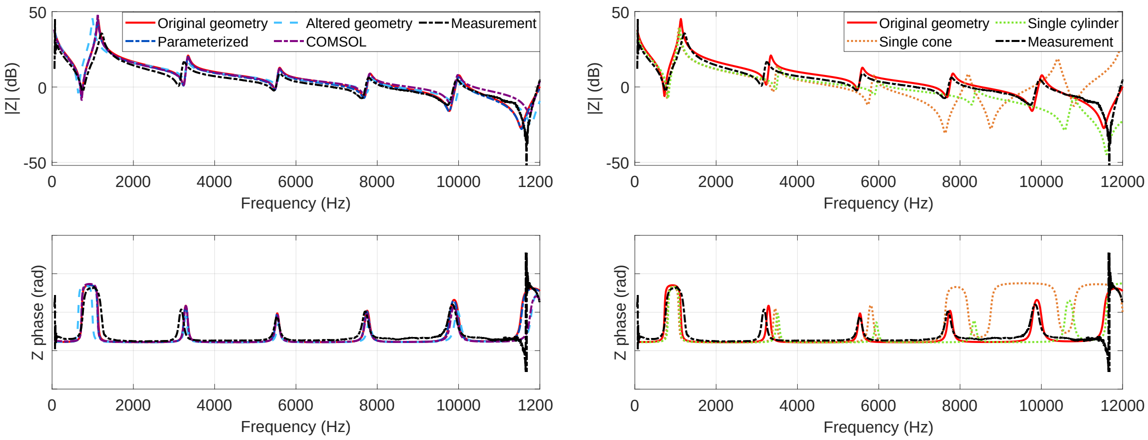

Figure 7: A comparison of the impedance (magnitude and phase) calculated from several possible methods of defining the mouthpiece geometry with an impedance measurement. This is for a mouthpiece closed at the outlet. In the left panel, the TMM calculation and the impedance measurement are shown (red and black curves) along with the calculation for the parameterized shape described in §3.B.i, the modified parameterization (light blue – note the deviation in the peak around 1000 Hz) whose geometry is shown as the green curve in Fig. 3, and the FEM (COMSOL) calculation described in §2.B. The right panel shows the same TMM calculation and measurement (red and black curves, as in the left panel), along with the calculations arising from the approximated cup shapes described in §3.B.ii and shown in Fig. 4. Note the progressively greater deviations in the orange and green curves as the frequency increases.

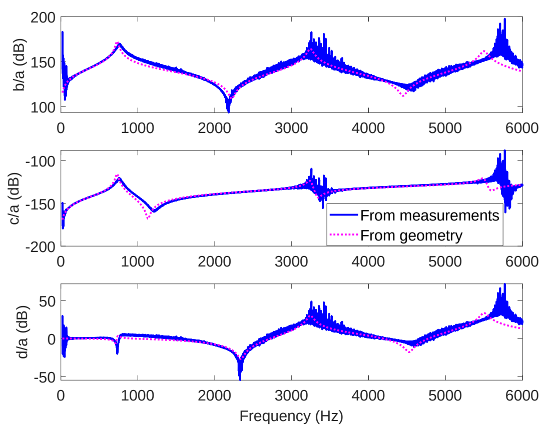

Figure 8: A comparison of the TMM element ratios of a mouthpiece from impedance measurements and calculated from the geometry.

C. BELL IMPEDANCE

The results of the models listed in §3.C and the comparison to the measured impedance are shown in Fig. 10. It can be seen in the top panel that the calculations that best match the measurements are the FEM (COMSOL) calculation (4) and the TMM calculation with a pulsating sphere as the radiation model and adjusted segment lengths to account for spherical wave propagation (3), which are the purple and yellow curves, respectively. Those curves are not easily visible in the top panel because they lie directly beneath the measured curve.

In the phase graph in the lower panel of Fig. 10, it can be seen from a visual examination that there is a linear drift between the measured and modeled data. Unfortunately, the cause of this is not clear, because two different impedance probes have been used to make the same measurement, and these agree in phase, and the TMM and FEM calculations also agree with each other. An investigation into this is ongoing.

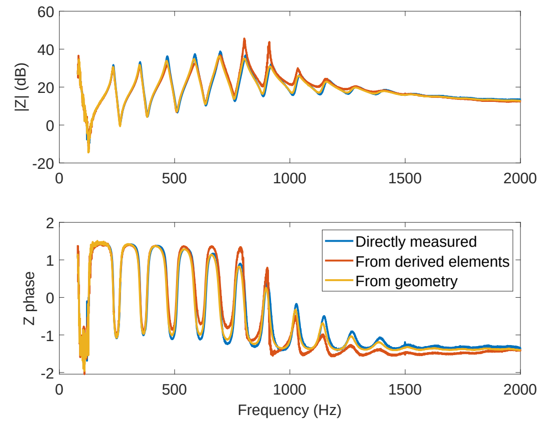

Figure 9: A comparison of the trumpet impedance (magnitude and phase) calculated from derived TMM elements (from impedance measurements involving the mouthpiece, as described in the text) and a measured trumpet load impedance, from a TMM calculation combined with the same load impedance, and from a direct impedance measurement of the same mouthpiece and trumpet.

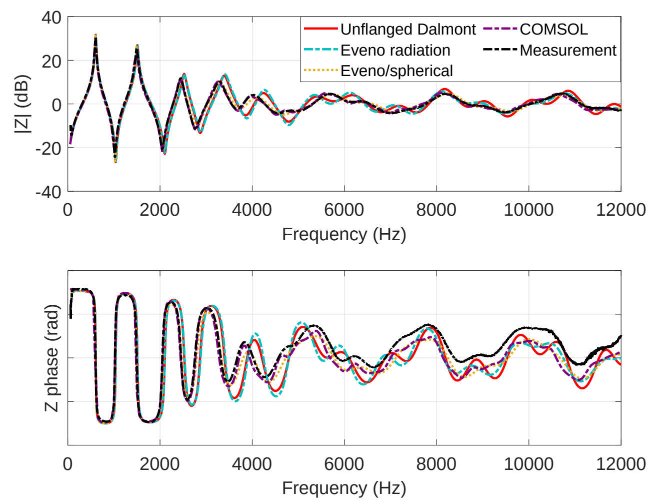

Figure 10: A comparison of the bell impedance calculated in several ways compared with impedance measurements. In the top panel (impedance magnitude), note the close match between the model incorporating the pulsating sphere radiation model with adjusted segment lengths (yellow curve) and the FEM calculation (purple curve) and with the impedance measurement (black curve). In the bottom panel (impedance phase), note the similar qualitative shapes of the yellow, purple, and black curves, but the increasing phase deviation between calculation and measurement with increasing frequencies, suggesting a constant or near-constant time delay.

5. DISCUSSION

As has been shown previously (e.g., Wang et al., 2021), the TMM calculation consistently qualitatively matches the performance of the FEM calculation for matching impedance measurements, insofar as is apparent from a visual comparison of the graphs. Moreover, even with the Bessel function calculations used for the losses, the TMM calculations take only a second or two for evaluations every 1 Hz, whereas the FEM calculations with evaluations every 50 Hz take a few minutes or more, depending on the physical size of the simulation.

The measured load impedance of an instrument has been shown in §4.A to be useful and reasonably accurate when a mouthpiece geometry is known and is combined with an instrument. This would be useful for testing multiple mouthpiece geometries with an instrument for which the geometry is not known but for which there is an input impedance measurement of the instrument with a cylindrical adaptor that can be used to calculate the load impedance.

It can be seen from Fig. 7 that there is some significant deviation between the measured and calculated input impedance of a mouthpiece, particularly in the peaks below 5 kHz. The relative uncertainty in measuring the mouthpiece geometry is likely to account for some of the deviation, but a more detailed examination of this is clearly required if the goal is to obtain an accurate estimation of the impedance from the mouthpiece geometry. One possible test is to use a 3D printed mouthpiece shape so that the geometry is more accurately known.

The parameterization of mouthpiece geometry presented in §3.B.i has been shown to be an effective approximation of measured trumpet mouthpiece geometries. Obviously, this will still need to be verified for more than just two mouthpieces, and for the mouthpieces of other brass instruments. In particular, a parameterization of horn mouthpieces would likely require differently defined parameters because of the more funnel-like shape.

The calculation of TMM elements from input impedance measurements described in §3.B.iii still requires some refinement. It is likely that the discrepancies seen in Figs. 8 and 9 arose, at least in part, because the end conditions of the cylindrical adaptor were not exactly matched to the end conditions for the mouthpiece, resulting in an imprecise calculation of the load impedance. The load impedances are very important for the calculation, so it will be necessary to either match the end conditions nearly perfectly, or to find a way to model the load impedances for the mouthpiece measurements. The closed condition could be assumed to have infinite load impedance, but that assumption does not improve the final result. Based on the available information, it is most likely that the uncertainty arises from the load impedance calculation corresponding to the anechoic measurement, so it will be necessary to find ways to mitigate this.

The results of the bell study given in §4.C confirm the results of Eveno et al. (2012), but these are still collectively only for trumpets and trombones, which have similarly shaped bells. It would be fruitful to further confirm with other brass instrument bells with different shapes.

The results presented here suggest that once the remaining areas of challenging geometry in brass instruments have been successfully modeled, including valves and curved pipes, it will be possible to calculate the input impedances of full instruments without resorting to approximating their geometries. This ability to assemble "virtual" instruments will be very useful in the future to brass instrument makers, designers, and researchers.

ACKNOWLEDGMENTS

This research was supported by an NSERC CGS funding award and by the Centre for Interdisciplinary Research in Music Media and Technology (CIRMMT). The authors would also like to thank Cristian Bosc for useful mouthpiece data.

REFERENCES

Ayers, R. D. (1996). "Impulse responses for feedback to the driver of a musical wind instrument". *The Journal of the Acoustical Society of America*, 100(2), 1190–1198.

Backus, J. (1977). *The Acoustical Foundations of Music*. Norton, New York, second edition.

Campbell, M., Myers, A., and Chick, J. (2013). "Influence of the bell profile of the trombone on sound reflection and radiation". *Proceedings of Meetings on Acoustics*, 19(1), 035068.

Chaigne, A. and Kergomard, J. (2016). *Acoustics of musical instruments*. Springer, New York.

Cremer, L. (1948). “On the acoustic boundary layer outside a rigid wall”. *Arch. Elektr. Uebertr*, 2, 235.

Dalmont, J.-P. (2001). “Acoustic Impedance Measurement, Part I: A Review”. *Journal of Sound and Vibration*, 243(3), 427–439.

Eveno, P., Dalmont, J.-P., Caussé, R., and Gilbert, J. (2012). “Wave Propagation and Radiation in a Horn: Comparisons Between Models and Measurements”. *Acta Acustica united with Acustica*, 98(1), 158–165.

Hélie, T. and Rodet, X. (2003). “Radiation of a Pulsating Portion of a Sphere: Application to Horn Radiation”. *Acta Acustica united with Acustica*, 89(4), 565–577.

Jansson, E. V. and Benade, A. H. (1974). “On plane and spherical waves in horns with non-uniform flare II. Prediction and measurements of resonance frequencies and radiation losses”. *Acta Acustica united with Acustica*, 31(4), 185–202.

Keefe, D. H. (1984). “Acoustical wave propagation in cylindrical ducts: Transmission line parameter approximations for isothermal and nonisothermal boundary conditions”. *The Journal of the Acoustical Society of America*, 75(1), 58–62.

Lefebvre, A. and Scavone, G. (2011). “A comparison of saxophone impedances and their playing behaviour”. *Proceedings of Forum Acusticum*, pages 539–544.

Macaluso, C. A. and Dalmont, J.-P. (2011). “Trumpet with near-perfect harmonicity: Design and acoustic results”. *The Journal of the Acoustical Society of America*, 129(1), 404–414.

Mignot, R., Helie, T., and Matignon, D. (2010). “Digital Waveguide Modeling for Wind Instruments: Building a State–Space Representation Based on the Webster–Lokshin Model”. *IEEE Transactions on Audio, Speech, and Language Processing*, 18(4), 843–854.

Plitnik, G. R. and Lawson, B. A. (1999). “An investigation of correlations between geometry, acoustic variables, and psychoacoustic parameters for French horn mouthpieces”. *The Journal of the Acoustical Society of America*, 106(2), 1111–1125.

Poirson, E., Petiot, J.-F. c., and Gilbert, J. (2005). “Study of the brightness of trumpet tones”. *The Journal of the Acoustical Society of America*, 118(4), 2656–2666.

Pyle, R. W. (1975). “Effective length of horns”. *The Journal of the Acoustical Society of America*, 57(6), 1309–1317.

Wang, S., Maestre, E., and Scavone, G. (2021). “Acoustical modeling of the saxophone mouthpiece as a transfer matrix”. *The Journal of the Acoustical Society of America*, 149(3), 1901–1912.

Webster, J. C. (1949). “Internal Tuning Differences due to Players and the Taper of Trumpet Bells”. *The Journal of the Acoustical Society of America*, 21(3), 208–214.

Zicari, M., MacRitchie, J., Ghirlanda, L., Vanchieri, A., Montorfano, D., Barbato, M. C., and Soldini, E. (2013). “Trumpet mouthpiece manufacturing and tone quality”. *The Journal of the Acoustical Society of America*, 134(5), 3872–3886.